

Analytic decay width of $H \rightarrow gg$ at order α_s^3 with full bottom quark mass dependence

Jian Wang^{a,b}, Yefan Wang^{c,d}

^a*School of Physics, Shandong University, Jinan, Shandong 250100, China*

^b*Center for High Energy Physics, Peking University, Beijing 100871, China*

^c*Department of Physics and Institute of Theoretical Physics, Nanjing Normal University,
Nanjing, Jiangsu 210023, China*

^d*Nanjing Key Laboratory of Particle Physics and Astrophysics, Nanjing Normal University,
Nanjing, Jiangsu 210023, China*

Abstract

Given the increasing precision of experimental measurements and the growing need for equally precise theoretical predictions, we provide in this paper an analytic calculation of the Higgs boson to gluons decay width up to next-to-leading order in quantum chromodynamics, i.e., order α_s^3 with α_s being the strong coupling, including full dependence on the bottom quark mass. Our results improve the theoretical understanding of this process, such as the logarithms in the small bottom quark mass limit, and provide an accurate prediction for the decay width that can be compared with experimental measurements.

1 Introduction

The discovery of the Higgs boson at the Large Hadron Collider (LHC) in 2012 marked a monumental achievement in particle physics, completing the Standard Model (SM) and opening a new era of precision measurements. Since then, extensive efforts have been made to measure the Higgs boson's properties, particularly its couplings to other SM particles. Current experimental results from the ATLAS and CMS collaborations at the LHC have provided significant constraints on these couplings, with uncertainties ranging from a few percent for the massive gauge bosons to tens of percent for the massive fermions [1]. Future colliders, such as the High-Luminosity LHC (HL-LHC) and proposed electron-positron colliders, aim to achieve percent-level precision or better in measuring these couplings [2]. Such precision will be crucial for testing the SM predictions and probing potential new physics beyond the Standard Model (BSM).

Among the various decay channels of the Higgs boson, the decay to gluons, $H \rightarrow gg$, plays a particularly important role. It is the third-largest decay mode, only next to $H \rightarrow bb$ and $H \rightarrow WW^*$ decays. In addition, it is sensitive to the same new physics as the dominant production mode $gg \rightarrow H$. At future lepton colliders, the signal strength of $H \rightarrow gg$ can be measured with a statistical uncertainty of 1.56% after the integrated luminosity reaches 5.6 fb^{-1} [3], which calls for a precision prediction on the decay. This process occurs at the leading order (LO) through a loop of heavy quarks, primarily the top quark due to its large Yukawa coupling. Theoretical predictions for this decay have been extensively studied. When the top quark is taken infinitely heavy and all the other quarks are assumed massless, the partial decay width has been calculated up to $\mathcal{O}(\alpha_s^5)$ [4, 5]. However, the result is only available up to $\mathcal{O}(\alpha_s^2)$ for massive bottom quarks [6].

While the bottom quark contribution is suppressed by its smaller Yukawa coupling, it is non-negligible in precision calculations, particularly in scenarios where BSM physics could alter the relative contributions of different quark flavors. It is also important to study the contributions induced by the bottom quark Yukawa coupling from a theoretical point of view. The bottom quark loop gives rise to double logarithms $\log^2(m_H^2/m_b^2)$, which have aroused considerable interest. For example, the structures of such logarithms at all orders have been derived from soft-collinear effective theory for the Higgs-gluon-gluon form factor [7]. An analytical calculation of the $H \rightarrow gg$ decay width at higher orders would help to understand the logarithmic structure for more physical observables than form factors.

2 Calculation framework

In our study, we consider that the $H \rightarrow gg$ decay is induced by two effective operators,

$$\mathcal{O}_1 = HG_{a,\mu\nu}G^{a,\mu\nu}, \quad \mathcal{O}_2 = m_b H \bar{b}b, \quad (1)$$

where the heavy top quark effects have been integrated out at leading power of $x \equiv m_H^2/m_t^2$ and contained in the Wilson coefficients of the effective operators [8–11]

$$C_1 = -\left(\frac{\alpha_s}{\pi}\right) \frac{1}{12} - \left(\frac{\alpha_s}{\pi}\right)^2 \frac{11}{48} - \left(\frac{\alpha_s}{\pi}\right)^3 \left[\frac{2777}{3456} + \frac{19}{192}L_t - n_f \left(\frac{67}{1152} - \frac{1}{36}L_t \right) \right] + \mathcal{O}(\alpha_s^4), \quad (2)$$

$$C_2 = 1 + \left(\frac{\alpha_s}{\pi}\right)^2 \left[\frac{5}{18} - \frac{1}{3}L_t \right] + \left(\frac{\alpha_s}{\pi}\right)^3 \left[-\frac{841}{1296} + \frac{5}{3}\zeta(3) - \frac{79}{36}L_t - \frac{11}{12}L_t^2 + n_f \left(\frac{53}{216} + \frac{1}{18}L_t^2 \right) \right] + \mathcal{O}(\alpha_s^4) \quad (3)$$

with $L_t = \log(\mu^2/m_t^2)$ and m_t being the top quark mass in the on-shell scheme. In the above expressions, the color factors $C_F = 4/3$, $C_A = 3$, $T_R = 1/2$ have been substituted while the

number of active quark flavors in this effective theory is still denoted by n_f . The m_H^2/m_t^2 power suppressed contribution to the $H \rightarrow gg$ decay rate has been estimated at $\mathcal{O}(\alpha_s^2)$ and turns out to be around 6% [6, 12].

According to the combination structure of effective operators in the squared amplitudes, the decay width of $H \rightarrow gg$ can be decomposed into three parts, i.e.,

$$\Gamma_{H \rightarrow gg} = \Gamma_{H \rightarrow gg}^{C_1 C_1} + \Gamma_{H \rightarrow gg}^{C_1 C_2} + \Gamma_{H \rightarrow gg}^{C_2 C_2}. \quad (4)$$

Each of them can be expanded in a series of the strong coupling α_s ,

$$\begin{aligned} \Gamma_{H \rightarrow gg}^{C_1 C_1} &= C_1 C_1 \left[\Delta_{0,gg}^{C_1 C_1} + \left(\frac{\alpha_s}{\pi} \right) \Delta_{1,gg}^{C_1 C_1} + \mathcal{O}(\alpha_s^2) \right], \\ \Gamma_{H \rightarrow gg}^{C_1 C_2} &= C_1 C_2 \left[\left(\frac{\alpha_s}{\pi} \right) \Delta_{1,gg}^{C_1 C_2} + \left(\frac{\alpha_s}{\pi} \right)^2 \Delta_{2,gg}^{C_1 C_2} + \mathcal{O}(\alpha_s^3) \right], \\ \Gamma_{H \rightarrow gg}^{C_2 C_2} &= C_2 C_2 \left[\left(\frac{\alpha_s}{\pi} \right)^2 \Delta_{2,gg}^{C_2 C_2} + \left(\frac{\alpha_s}{\pi} \right)^3 \Delta_{3,gg}^{C_2 C_2} + \mathcal{O}(\alpha_s^4) \right], \end{aligned} \quad (5)$$

where we have written down explicitly the terms needed to obtain $\Gamma_{H \rightarrow gg}$ up to $\mathcal{O}(\alpha_s^3)$.

We compute the decay width of $H \rightarrow gg$ via the optical theorem, i.e.,

$$\Gamma_{H \rightarrow gg} = \frac{\text{Im}_{gg}(\Sigma)}{m_H}, \quad (6)$$

where Σ represents the amplitude of the process $H \rightarrow gg \rightarrow H$. The typical Feynman diagrams are shown in figure 1. The notation Im_{gg} denotes that only the imaginary part from a cut on at least two gluons or one gluon and one light quark pair is retained. Explicitly, we consider the cuts on gg , ggg and $gq\bar{q}$, where q represents the light quarks. Note that the $b\bar{b}g$ and $b\bar{b}gg$ final states are assigned to the contribution to $H \rightarrow b\bar{b}$. The calculation method, including the renormalization procedure, can be found in our previous papers [13, 14]. Below we present the main results.

3 Full results of $\Delta_{i,gg}^{C_1 C_1}$, $\Delta_{i,gg}^{C_1 C_2}$, and $\Delta_{i,gg}^{C_2 C_2}$

Because the coefficient C_1 starts at $\mathcal{O}(\alpha_s)$, we only need to compute one- and two-loop $H \rightarrow gg \rightarrow H$ diagrams with two \mathcal{O}_1 operators to obtain $\Gamma_{H \rightarrow gg}^{C_1 C_1}$ up to $\mathcal{O}(\alpha_s^3)$; see diagrams (a,b,c) in figure 1. The imaginary part of the one-loop diagram gives the result of $\Delta_{0,gg}^{C_1 C_1}$,

$$\Delta_{0,gg}^{C_1 C_1} = \frac{C_A C_F m_H^3}{2\pi v^2}. \quad (7)$$

where v is the vacuum expectation value. And the two-loop calculation leads to

$$\begin{aligned} \Delta_{1,gg}^{C_1 C_1} &= \frac{m_H^3}{\pi v^2} C_A C_F \left(\left[-\frac{1}{6} \log(z) - \frac{1}{6} \log\left(\frac{\mu^2}{m_H^2}\right) \right] \right. \\ &\quad \left. + C_A \left[\frac{11}{12} \log\left(\frac{\mu^2}{m_H^2}\right) + \frac{73}{24} \right] + n_l \left[-\frac{1}{6} \log\left(\frac{\mu^2}{m_H^2}\right) - \frac{7}{12} \right] \right). \end{aligned} \quad (8)$$

Here we define the dimensionless variable $z \equiv m_H^2/m_b^2$ with m_b being the bottom quark mass in the on-shell scheme. The first term comes from the massive bottom quark loop. Although it has a logarithmic structure, it does not dominate the correction $\Delta_{1,gg}^{C_1 C_1}$ because of the small coefficient. We have used $n_l = n_f - 1$ to denote the number of massless quark flavors.

The result of $\Delta_{1,gg}^{C_1 C_2}$ is obtained by calculating the imaginary part of two-loop diagrams with one \mathcal{O}_1 and one \mathcal{O}_2 operators, as shown in figure 1(d). We obtain

$$\Delta_{1,gg}^{C_1 C_2} = \frac{m_H m_b \bar{m}_b}{\pi v^2} C_A C_F \left(\frac{z-4}{8z} \left[\log^2 \left(\frac{1}{2} (z - \sqrt{(z-4)z} - 2) \right) - \pi^2 \right] - \frac{1}{2} \right), \quad (9)$$

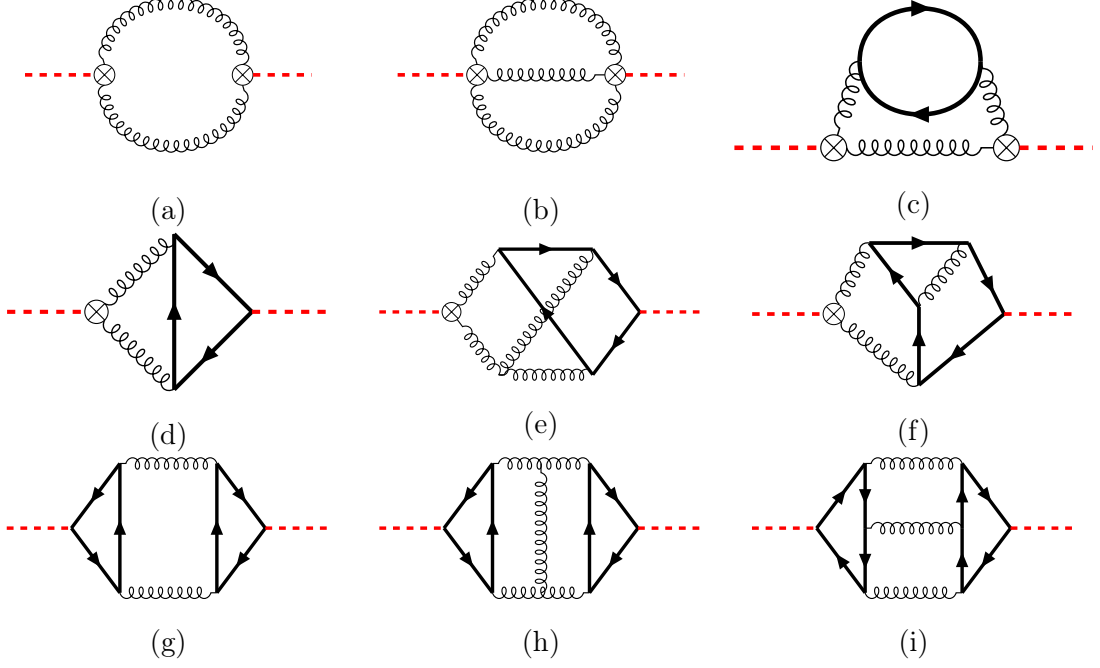


Figure 1: Sample Feynman diagrams contributing to $\Delta_{i,gg}^{C_1C_1}$, $\Delta_{i,gg}^{C_1C_2}$ and $\Delta_{i,gg}^{C_2C_2}$. (a) is the one-loop diagram of $\Delta_{0,gg}^{C_1C_1}$ and (b)-(c) are the two-loop diagrams of $\Delta_{1,gg}^{C_1C_1}$. (d) is the two-loop diagram of $\Delta_{1,gg}^{C_1C_2}$ and (e)-(f) are the three-loop diagrams of $\Delta_{2,gg}^{C_1C_2}$. (g) is the three-loop diagram of $\Delta_{2,gg}^{C_2C_2}$ and (h)-(i) are the four-loop diagrams of $\Delta_{3,gg}^{C_2C_2}$. The thick black and red lines denote the massive bottom quark and the Higgs boson, respectively.

where the factor $\overline{m_b}$ comes from the Yukawa coupling renormalized in the $\overline{\text{MS}}$ scheme while m_b arises from the propagator. The evaluation of corresponding three-loop diagrams, e.g., the figure 1(e,f), gives the result

$$\begin{aligned}
\Delta_{2,gg}^{C_1C_2} \Big|_{\mu=m_H} &= \frac{m_H m_b \overline{m_b}}{\pi v^2} \frac{1}{(w-1)^2} \times \\
&\left(\left[32G(0,0,1,0,w) - 64G(0,-1,0,0,w) + 128G(0,0,-1,0,w) - 112G(0,1,0,0,w) \right. \right. \\
&+ 64\pi^2 G(0,-1,w) + 112\pi^2 G(0,1,w) + 64i\pi G(0,-1,0,w) - 128i\pi G(0,0,-1,w) \\
&- 32i\pi G(0,0,1,w) + 112i\pi G(0,1,0,w) + 64\zeta(3)G(0,w) - 7n_l G(0,w) - 64i\pi\zeta(3) \\
&+ 7i\pi n_l \left. \right] \frac{(w+1)(w^2+1)}{12(w-1)} + \left[12G(0,0,1,w) - 48G(0,-1,0,w) - 6G(1,0,0,w)n_l \right. \\
&+ 3n_l G(0,0,0,w) + 48i\pi G(0,-1,w) + 6i\pi G(1,0,w)n_l - 3i\pi n_l G(0,0,w) - 3\pi^2 n_l G(0,w) \\
&+ 6\pi^2 n_l G(1,w) - 6n_l \zeta(3) + 2i\pi^3 n_l \left. \right] \frac{(w+1)^2}{9} \\
&+ \left[G(1,0,0,w) - i\pi G(1,0,w) - \pi^2 G(1,w) \right] \frac{57w^2 + 122w + 57}{3} \\
&+ \left[G(0,0,w) - i\pi G(0,w) - \pi^2 \right] \frac{127w^4 - 128w^3 - 612w^2 - 128w + 127}{8(w-1)^2} \\
&- \left[G(0,0,w) - i\pi G(0,w) - \pi^2 \right] \frac{n_l (5w^4 - 31w^2 + 5)}{9(w-1)^2} \\
&+ \left[G(0,0,0,0,w) - i\pi G(0,0,0,w) \right] \frac{13w^4 - 54w^3 - 72w^2 - 54w + 5}{6(w-1)^2}
\end{aligned}$$

$$\begin{aligned}
& - \left[G(0,0,0,w) - i\pi G(0,0,w) \right] \frac{141w^3 + 205w^2 - 7w - 39}{12(w-1)} \\
& - \frac{\pi^2 (31w^4 - 162w^3 - 216w^2 - 162w + 23) G(0,0,w)}{18(w-1)^2} - \frac{8(w-1)^2 G(1,w)}{3} \\
& + \left[(w-1) (391w^3 + 583w^2 + 11w - 85) + 36i\pi (w^4 - 6w^3 - 8w^2 - 6w + 1) \right] \frac{\pi^2 G(0,w)}{36(w-1)^2} \\
& - \frac{\pi^4 (-31w^4 + 270w^3 + 360w^2 + 270w - 59)}{90(w-1)^2} + \frac{(37w^2 + 82w + 37) \zeta(3)}{3} \\
& - \frac{i\pi^3 (125w^3 + 189w^2 + 9w - 23)}{18(w-1)} + \frac{(233w^2 - 382w + 233) n_l}{72} \\
& + \frac{-6217w^2 + 8750w - 6217}{96} \Big), \tag{10}
\end{aligned}$$

where w is determined by

$$r = \sqrt{z(z-4)}, \quad z = -\frac{(w-1)^2}{w}, \quad -1 < w < 0. \tag{11}$$

For simplicity, the color factors $C_F = 4/3$, $C_A = 3$, $T_R = 1/2$ have been substituted. The multiple polylogarithm (MPL) [15] is defined by $G(w) \equiv 1$ and

$$G(l_1, l_2, \dots, l_n, w) \equiv \int_0^w \frac{dt}{t-l_1} G(l_2, \dots, l_n, t), \tag{12}$$

$$G(\vec{0}_n, w) \equiv \frac{1}{n!} \log^n w. \tag{13}$$

The third kind of contribution, $\Delta_{i,gg}^{C_2C_2}$, comes from the flavor singlet diagrams with two Yukawa couplings, as shown in figure 1(g,h,i). The helicity conservation along each fermion loop requires that an overall m_b factor appears for such a loop, and thus the results are highly suppressed by m_b^2/m_H^2 compared with the first two kinds of contributions. We present only the leading non-vanishing contribution below,

$$\begin{aligned}
\Delta_{2,gg}^{C_2C_2} &= -\frac{m_b^2 \overline{m_b}^2}{96\pi v^2 m_H} \frac{C_A}{(w-1)^4} \times \\
& \left[16(w^2-1)^2 \log^2(-w) - (4(w-1)^2 + \pi^2(w+1)^2 + (w+1)^2 \log^2(-w))^2 \right]. \tag{14}
\end{aligned}$$

4 Asymptotic expansion

In the small m_b , or $z \rightarrow \infty$, limit, the leading-order non-vanishing results in the C_1C_2 and C_2C_2 combinations can be expanded as

$$\begin{aligned}
\Delta_{1,gg}^{C_1C_2} |_{z \rightarrow \infty} &= \frac{m_H m_b \overline{m_b}}{\pi v^2} C_A C_F \times \\
& \left[\frac{1}{8} \log^2(z) - \frac{\pi^2}{8} - \frac{1}{2} - \frac{1}{2} \frac{\log^2(z)}{z} - \frac{1}{2} \frac{\log(z)}{z} + \frac{\pi^2}{2z} + \mathcal{O}(z^{-2}) \right], \tag{15}
\end{aligned}$$

$$\begin{aligned}
\Delta_{2,gg}^{C_2C_2} |_{z \rightarrow \infty} &= \frac{m_b^2 \overline{m_b}^2}{\pi v^2 m_H} C_A \times \\
& \left[\frac{(\log^2(z) - 4\log(z) + \pi^2 + 4) (\log^2(z) + 4\log(z) + \pi^2 + 4)}{96} + \mathcal{O}(z^{-1}) \right]. \tag{16}
\end{aligned}$$

where we have kept the terms up to $\mathcal{O}(z^{-2})$ after considering the coefficients. The logarithms arise from the soft or collinear bottom quarks from the expansion-by-region point of view. At the

current perturbative orders, the above results correspond to the decay $H \rightarrow gg$ with a bottom quark loop. The two final-state gluons move back-to-back in the center-of-mass frame of the Higgs boson. In the method of regions, the momentum of the internal bottom quark could be collinear to either of the external gluons or soft with respect to the gluon momenta.

The next-to-leading order correction in the $C_1 C_2$ combination is expanded to

$$\begin{aligned}
\Delta_{2,gg}^{C_1 C_2}|_{z \rightarrow \infty} &= \frac{m_H m_b \overline{m_b}}{\pi v^2} \times \\
&\left\{ C_A^2 C_F \left[\frac{1}{192} \log^4(z) + \frac{13}{288} \log^3(z) + \frac{11}{48} \log\left(\frac{\mu^2}{m_H^2}\right) \log^2(z) - \frac{\pi^2}{32} \log^2(z) + \frac{349}{576} \log^2(z) \right. \right. \\
&- \frac{13\pi^2}{96} \log(z) + \frac{115}{192} \log(z) - \frac{11\pi^2}{48} \log\left(\frac{\mu^2}{m_H^2}\right) - \frac{11}{12} \log\left(\frac{\mu^2}{m_H^2}\right) + \frac{\pi^4}{192} + \frac{11\zeta(3)}{12} \\
&- \frac{349\pi^2}{576} - \frac{5321}{1152} + \frac{1}{96} \frac{\log^4(z)}{z} - \frac{7}{18} \frac{\log^3(z)}{z} - \frac{11}{12} \log\left(\frac{\mu^2}{m_H^2}\right) \frac{\log^2(z)}{z} - \frac{\pi^2 \log^2(z)}{16z} \\
&- \frac{89 \log^2(z)}{72z} + \frac{7\pi^2 \log(z)}{6z} - \frac{11}{12} \log\left(\frac{\mu^2}{m_H^2}\right) \frac{\log(z)}{z} - \frac{425 \log(z)}{72z} + \frac{11\pi^2}{12z} \log\left(\frac{\mu^2}{m_H^2}\right) \\
&\left. + \frac{\pi^4}{96z} - \frac{17\zeta(3)}{3z} + \frac{89\pi^2}{72z} + \frac{35}{12z} \right] \\
&+ C_A C_F^2 \left[-\frac{1}{192} \log^4(z) + \frac{1}{32} \log^3(z) - \frac{\pi^2}{96} \log^2(z) + \frac{3}{32} \log\left(\frac{\mu^2}{m_H^2}\right) \log^2(z) + \frac{1}{8} \log^2(z) \right. \\
&+ \zeta(3) \log(z) + \frac{13\pi^2}{96} \log(z) + \frac{3}{8} \log(z) - \frac{3\pi^2}{32} \log\left(\frac{\mu^2}{m_H^2}\right) - \frac{3}{8} \log\left(\frac{\mu^2}{m_H^2}\right) + \frac{23\pi^4}{960} \\
&+ \frac{\zeta(3)}{4} - \frac{\pi^2}{8} - \frac{7}{4} + \frac{1}{48} \frac{\log^4(z)}{z} + \frac{3 \log^3(z)}{8z} - \frac{3}{8} \log\left(\frac{\mu^2}{m_H^2}\right) \frac{\log^2(z)}{z} + \frac{\pi^2 \log^2(z)}{24z} \\
&- \frac{1 \log^2(z)}{4z} - 4\zeta(3) \frac{\log(z)}{z} - \frac{15\pi^2 \log(z)}{8z} - \frac{3}{8} \log\left(\frac{\mu^2}{m_H^2}\right) \frac{\log(z)}{z} - \frac{3 \log(z)}{2z} \\
&\left. + \frac{3\pi^2}{8z} \log\left(\frac{\mu^2}{m_H^2}\right) - \frac{23\pi^4}{240z} + \frac{\zeta(3)}{z} - \frac{5\pi^2}{24z} - \frac{4}{z} \right] \\
&+ C_A C_F n_l \left[-\frac{1}{72} \log^3(z) - \frac{1}{24} \log\left(\frac{\mu^2}{m_H^2}\right) \log^2(z) - \frac{5}{72} \log^2(z) + \frac{\pi^2}{24} \log(z) - \frac{7}{48} \log(z) \right. \\
&+ \frac{\pi^2}{24} \log\left(\frac{\mu^2}{m_H^2}\right) + \frac{1}{6} \log\left(\frac{\mu^2}{m_H^2}\right) - \frac{\zeta(3)}{6} + \frac{5\pi^2}{72} + \frac{233}{288} \\
&+ \frac{1}{18} \frac{\log^3(z)}{z} + \frac{1}{6} \log\left(\frac{\mu^2}{m_H^2}\right) \frac{\log^2(z)}{z} + \frac{5}{18} \frac{\log^2(z)}{z} + \frac{1}{6} \log\left(\frac{\mu^2}{m_H^2}\right) \frac{\log(z)}{z} - \frac{\pi^2 \log(z)}{6z} \\
&\left. + \frac{25 \log(z)}{36z} - \frac{\pi^2}{6z} \log\left(\frac{\mu^2}{m_H^2}\right) + \frac{2\zeta(3)}{3z} - \frac{5\pi^2}{18z} - \frac{1}{6z} \right] \\
&+ C_A C_F \left[-\frac{1}{24} \log^3(z) - \frac{1}{24} \log\left(\frac{\mu^2}{m_H^2}\right) \log^2(z) + \frac{\pi^2}{24} \log^2(z) + \frac{1}{6} \log(z) + \frac{\pi^2}{24} \log\left(\frac{\mu^2}{m_H^2}\right) \right. \\
&+ \frac{1}{6} \log\left(\frac{\mu^2}{m_H^2}\right) + \frac{1}{6} \frac{\log^3(z)}{z} + \frac{1}{6} \log\left(\frac{\mu^2}{m_H^2}\right) \frac{\log^2(z)}{z} + \frac{1}{6} \frac{\log^2(z)}{z} + \frac{1}{6} \log\left(\frac{\mu^2}{m_H^2}\right) \frac{\log(z)}{z} \\
&\left. - \frac{\pi^2 \log(z)}{6z} - \frac{\pi^2}{6z} \log\left(\frac{\mu^2}{m_H^2}\right) \right] \Bigg\}, \tag{17}
\end{aligned}$$

where we retain all color structures explicitly. The ratio of the $\log^4(z)$ term in $\Delta_{2,gg}^{C_1 C_2}$ over the $\log^2(z)$ term in $\Delta_{1,gg}^{C_1 C_2}$ reads

$$\frac{C_A - C_F}{24}. \tag{18}$$

This factor agrees with the analysis of the Hgg form factor after proper subtraction of infrared divergences in refs. [7, 16]¹, representing a general color factor for the subleading power contribution induced by a soft quark. The ratio of the $\log^4(z)/z$ term in $\Delta_{2,gg}^{C_1C_2}$ over the $\log^2(z)/z$ term in $\Delta_{1,gg}^{C_1C_2}$ is given by

$$-\frac{2C_F + C_A}{48}, \quad (19)$$

which differs from that in eq. (18). Therefore, a new resummation formula of the large logarithms at sub-subleading power is expected; see the discussion on the form factor in [17]. Besides the leading logarithms, we also provide all next-to-leading logarithmic structure, which would help to develop a resummation formalism at higher logarithmic level.

Summarizing the above results, we obtain the partial decay width for $H \rightarrow gg$

$$\begin{aligned} \Gamma_{H \rightarrow gg} = & \frac{m_H^3}{v^2\pi} \left\{ \left(\frac{\alpha_s}{\pi} \right)^2 \frac{1}{72} + \left(\frac{\alpha_s}{\pi} \right)^3 \left[-\frac{1}{216} \log(\bar{z}) + \frac{229}{864} \right] \right\} \\ & + \frac{m_H \bar{m}_b^2}{v^2\pi} \left\{ \left(\frac{\alpha_s}{\pi} \right)^2 \left[-\frac{1}{24} \log^2(\bar{z}) + \frac{\pi^2}{24} + \frac{1}{6} \right] \right. \\ & + \left(\frac{\alpha_s}{\pi} \right)^3 \left[-\frac{5}{1728} \log^4(\bar{z}) - \frac{59}{864} \log^3(\bar{z}) + \frac{31\pi^2}{864} \log^2(\bar{z}) - \frac{989}{1728} \log^2(\bar{z}) \right. \\ & - \frac{4\zeta(3)}{9} \log(\bar{z}) + \frac{41\pi^2}{864} \log(\bar{z}) - \frac{137}{576} \log(\bar{z}) - \frac{137\pi^4}{8640} - \frac{29\zeta(3)}{36} \\ & \left. \left. + \frac{1277\pi^2}{1728} + \frac{17275}{3456} \right] + \mathcal{O}(\bar{z}^{-1}) \right\} \end{aligned} \quad (20)$$

where we have chosen $\mu = m_H$ and converted the on-shell mass to $\overline{\text{MS}}$ mass using the relation

$$\bar{m}_b = m_b \left\{ 1 - \frac{\alpha_s C_F}{\pi} \left[1 + \frac{3}{4} \log \left(\frac{\mu^2}{m_b^2} \right) \right] + \mathcal{O}(\alpha_s^2) \right\} \quad (21)$$

and defined $\bar{z} = m_H^2/\bar{m}_b^2$. Adding the result of $H \rightarrow b\bar{b}$ decay in our previous papers [13, 14], we obtain the decay width to all hadrons at leading power of m_b^2 ,

$$\begin{aligned} \Gamma_{H \rightarrow \text{hadrons}} = & \frac{m_H^3}{v^2\pi} \left\{ \left(\frac{\alpha_s}{\pi} \right)^2 \frac{1}{72} + \left(\frac{\alpha_s}{\pi} \right)^3 \frac{215}{864} + \mathcal{O}(\bar{z}^{-1}) \right\} \\ & + \frac{3m_H \bar{m}_b^2}{8v^2\pi} \left\{ 1 + \left(\frac{\alpha_s}{\pi} \right) \frac{17}{3} + \left(\frac{\alpha_s}{\pi} \right)^2 \left[-\frac{2}{3} \log(x) - \frac{97\zeta(3)}{6} - \frac{47\pi^2}{36} + \frac{9299}{144} \right] \right. \\ & + \left(\frac{\alpha_s}{\pi} \right)^3 \left[-\frac{23}{18} \log^2(x) - \frac{49}{6} \log(x) + \frac{1945\zeta(5)}{36} - \frac{5\pi^4}{108} - \frac{81703\zeta(3)}{216} \right. \\ & \left. \left. - \frac{10507\pi^2}{324} + \frac{38056609}{46656} \right] + \mathcal{O}(\bar{z}^{-1}) \right\} \\ & + \mathcal{O}(x) + \mathcal{O}(\alpha_s^4), \end{aligned} \quad (22)$$

which is consistent with the results [11, 18].

In the above equations, we have also taken the limit of $m_t \rightarrow \infty$, i.e., taken the result at leading power of $x \equiv m_H^2/m_t^2$. We compute the next-to-leading power contribution as shown in figure 2, and obtain

$$\Gamma_{H \rightarrow gg}^x = \frac{m_H^3 x}{v^2\pi} \left\{ \left(\frac{\alpha_s}{\pi} \right)^2 \left[\frac{7}{4320} + \frac{1}{\bar{z}} \left(-\frac{7}{2880} \log^2(\bar{z}) + \frac{7\pi^2}{2880} + \frac{7}{720} \right) \right] + \mathcal{O}(\bar{z}^{-2}) \right\}$$

¹Note that the finite part of the form factor depends on the infrared subtraction term. The product of the infrared subtraction term and the LO amplitude could induce leading logarithms. The agreement indicates that the $H \rightarrow ggg$ decay process does not provide leading logarithms once the infrared divergences are properly subtracted.

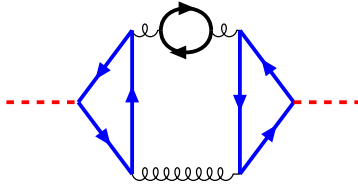


Figure 2: Sample Feynman diagrams contributing to the m_H^2/m_t^2 corrections. The blue and black lines denote the top and bottom quarks, respectively.

$$+ \left(\frac{\alpha_s}{\pi} \right)^3 \left[- \frac{7}{12960} \log(\bar{z}) + \frac{5431}{155520} + \mathcal{O}(\bar{z}^{-1}) \right] \} \quad (23)$$

where we have chosen $\mu = m_H$. The $\mathcal{O}(\alpha_s^3)$ correction is new, while the $\mathcal{O}(\alpha_s^2)$ correction can be found in [6, 19].

5 Numerical results

We calculate the decay width numerically by taking the input parameters

$$\begin{aligned} \bar{m}_b(\bar{m}_b) &= 4.18 \text{ GeV}, & m_b &= 5.07 \text{ GeV}, & m_H &= 125.09 \text{ GeV}, \\ m_t &= 172.69 \text{ GeV} & \alpha_s(m_Z) &= 0.1181, & G_F &= 1.166378 \times 10^{-5} \text{ GeV}^{-2}. \end{aligned} \quad (24)$$

The running bottom quark mass and strong coupling at other scales are determined using the package `RunDec` [20, 21], e.g., $\bar{m}_b(m_H) = 2.78425 \text{ GeV}$ and $\alpha_s(m_H) = 0.112715$. The contributions from various coupling combinations to the partial decay width are shown in table 1 in the on-shell and $\overline{\text{MS}}$ schemes, respectively.

At leading order, the C_1C_1 combination is dominant, while the C_1C_2 combination reduces the decay with by 13% (7%) in the on-shell ($\overline{\text{MS}}$) scheme. The correction from the C_2C_2 combination in the on-shell ($\overline{\text{MS}}$) scheme only amounts to 1% (0.2%) of that from C_1C_1 . This hierarchy in the magnitude does not agree with the power counting in z , which is around 0.1%. An enhancement from the logarithmic terms should be taken into account to understand the relative size. Since the contribution from the C_2C_2 combination is so small, it is reasonable to neglect its higher order corrections in phenomenological studies.

The NLO QCD correction in the C_1C_1 combination increases the LO result by around 61% and is insensitive to the mass schemes. The notable correction is not unexpected given that the QCD corrections in hadronic Higgs production at the LHC, which is related to $H \rightarrow gg$ decay by crossing symmetry, are also significant [22]. This behavior indicates that NNLO QCD corrections may be important. The result for the $H \rightarrow gg$ decay with massless bottom quarks was computed a long time ago, and a correction of 20% is found at NNLO [4, 5]. However, the result with massive bottom quarks is still missing. We leave such a study to future work.

The NLO QCD correction in the C_1C_2 combination is about 47% (88%) of the corresponding LO result in the on-shell ($\overline{\text{MS}}$) scheme. We have checked that the dominant corrections come from the logarithms of z . We show the contribution $\Gamma_{H \rightarrow gg}^{C_1C_2}$ and the full $H \rightarrow gg$ decay width at LO and NLO in figure 3. The renormalization scale and scheme dependencies are improved slightly after including the NLO QCD correction. Adding the power corrections of m_H^2/m_t^2 in (23), we obtain the results up to $\mathcal{O}(\alpha_s^3)$:

$$\Gamma_{H \rightarrow gg}^{\text{NLO}} (\text{on-shell}) = 0.278_{-0.033}^{+0.038} \text{ MeV}, \quad (25a)$$

$$\Gamma_{H \rightarrow gg}^{\text{NLO}} (\overline{\text{MS}}) = 0.289_{-0.031}^{+0.034} \text{ MeV}, \quad (25b)$$

where only the scale uncertainty is considered. The correction in (23) is only 7%, and therefore we expect the higher power effects to be around 4% at most.

| | | on-shell scheme | | | $\overline{\text{MS}}$ scheme | | |
|---------------------------|---------------------------------------|-----------------------|-------------|--------------|-------------------------------|-------------|--------------|
| [MeV] | | $\mu = \frac{m_H}{2}$ | $\mu = m_H$ | $\mu = 2m_H$ | $\mu = \frac{m_H}{2}$ | $\mu = m_H$ | $\mu = 2m_H$ |
| $\mathcal{O}(\alpha_s^2)$ | $\Gamma_{H \rightarrow gg}^{C_2 C_2}$ | 0.003208 | 0.002598 | 0.002148 | 0.0006336 | 0.0004269 | 0.0002994 |
| | $\Gamma_{H \rightarrow gg}^{C_1 C_2}$ | -0.03018 | -0.02444 | -0.02021 | -0.01601 | -0.01200 | -0.00925 |
| | $\Gamma_{H \rightarrow gg}^{C_1 C_1}$ | 0.2269 | 0.1837 | 0.1520 | 0.2269 | 0.1837 | 0.1520 |
| $\mathcal{O}(\alpha_s^3)$ | $\Gamma_{H \rightarrow gg}^{C_2 C_2}$ | - | - | - | - | - | - |
| | $\Gamma_{H \rightarrow gg}^{C_1 C_2}$ | -0.009250 | -0.01140 | -0.01208 | -0.01088 | -0.01054 | -0.009632 |
| | $\Gamma_{H \rightarrow gg}^{C_1 C_1}$ | 0.1052 | 0.1117 | 0.1104 | 0.1019 | 0.1091 | 0.1082 |

Table 1: The contributions $\Gamma_{H \rightarrow gg}^{C_2 C_2}$, $\Gamma_{H \rightarrow gg}^{C_1 C_2}$ and $\Gamma_{H \rightarrow gg}^{C_1 C_1}$ at different orders of α_s in the on-shell and $\overline{\text{MS}}$ schemes.

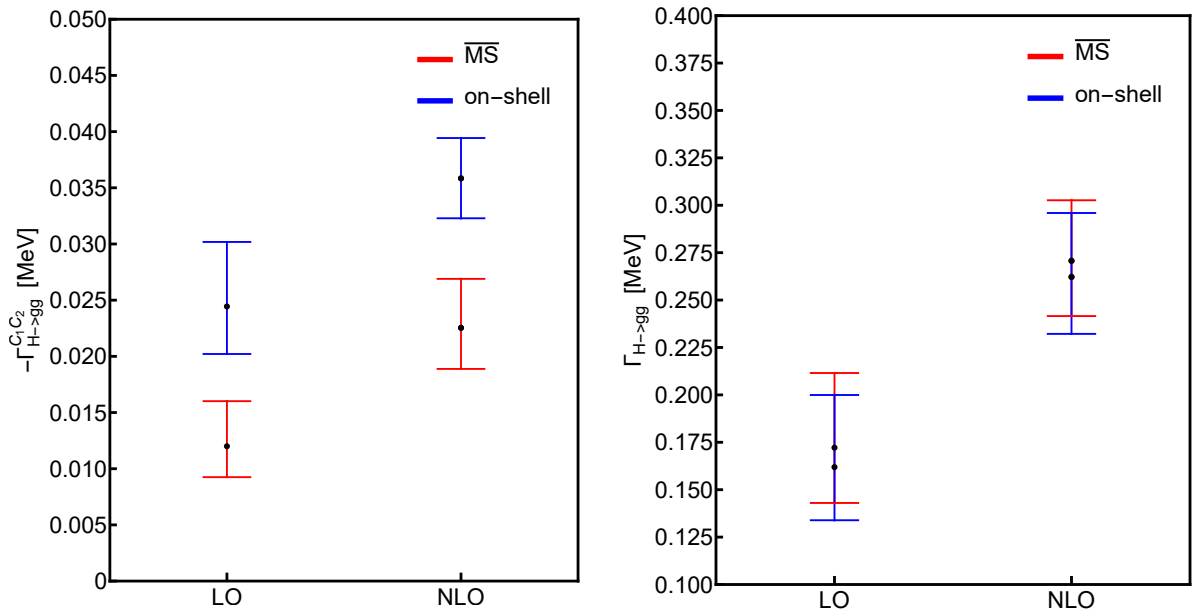


Figure 3: The contribution $\Gamma_{H \rightarrow gg}^{C_1 C_2}$ and full $\Gamma_{H \rightarrow gg}$ at different orders of α_s in the on-shell and $\overline{\text{MS}}$ schemes.

6 Conclusion

The Higgs boson decay into gluons is an important process because it is the third-largest decay mode. We calculate the decay width up to α_s^3 with full bottom quark mass dependence analytically. The results have been expressed in terms of MPLs. The asymptotic expansion in the small m_b limit exhibits intriguing features that are relevant to resummation of large logarithms at subleading power. Our numerical results show that the NLO QCD corrections increase the decay rate significantly, while the scale and scheme dependencies are improved only marginally. Combining with the power corrections of m_H^2/m_t^2 , we provide precise predictions on the decay width in both the on-shell and $\overline{\text{MS}}$ renormalization schemes of the bottom quark mass.

References

- [1] ATLAS collaboration, G. Aad et al., *Characterising the Higgs boson with ATLAS data from Run 2 of the LHC*, *Phys. Rept.* **11** (2024) 001, [2404.05498].
- [2] ATLAS collaboration, *Projections for measurements of Higgs boson cross sections, branching ratios, coupling parameters and mass with the ATLAS detector at the HL-LHC*, .
- [3] Y. Zhu, H. Cui and M. Ruan, *The Higgs $\rightarrow b\bar{b}, c\bar{c}$, gg measurement at CEPC*, *JHEP* **11** (2022) 100, [2203.01469].
- [4] K. G. Chetyrkin, B. A. Kniehl and M. Steinhauser, *Hadronic Higgs decay to order α_s^4* , *Phys. Rev. Lett.* **79** (1997) 353–356, [hep-ph/9705240].
- [5] P. A. Baikov and K. G. Chetyrkin, *Top Quark Mediated Higgs Boson Decay into Hadrons to Order α_s^5* , *Phys. Rev. Lett.* **97** (2006) 061803, [hep-ph/0604194].
- [6] K. G. Chetyrkin and A. Kwiatkowski, *Second order QCD corrections to scalar and pseudoscalar Higgs decays into massive bottom quarks*, *Nucl. Phys. B* **461** (1996) 3–18, [hep-ph/9505358].
- [7] Z. L. Liu, M. Neubert, M. Schnubel and X. Wang, *Factorization at next-to-leading power and endpoint divergences in $gg \rightarrow h$ production*, *JHEP* **06** (2023) 183, [2212.10447].
- [8] K. G. Chetyrkin, B. A. Kniehl and M. Steinhauser, *Three loop $O(\alpha_s^2 G(F) M(t)^2)$ corrections to hadronic Higgs decays*, *Nucl. Phys. B* **490** (1997) 19–39, [hep-ph/9701277].
- [9] K. G. Chetyrkin, B. A. Kniehl and M. Steinhauser, *Decoupling relations to $O(\alpha_s^3)$ and their connection to low-energy theorems*, *Nucl. Phys. B* **510** (1998) 61–87, [hep-ph/9708255].
- [10] T. Liu and M. Steinhauser, *Decoupling of heavy quarks at four loops and effective Higgs-fermion coupling*, *Phys. Lett. B* **746** (2015) 330–334, [1502.04719].
- [11] J. Davies, M. Steinhauser and D. Wellmann, *Completing the hadronic Higgs boson decay at order α_s^4* , *Nucl. Phys. B* **920** (2017) 20–31, [1703.02988].
- [12] M. Schreck and M. Steinhauser, *Higgs Decay to Gluons at NNLO*, *Phys. Lett. B* **655** (2007) 148–155, [0708.0916].
- [13] J. Wang, Y. Wang and D.-J. Zhang, *Analytic decay width of the Higgs boson to massive bottom quarks at next-to-next-to-leading order in QCD*, *JHEP* **03** (2024) 068, [2310.20514].
- [14] J. Wang, X. Wang and Y. Wang, *Analytic decay width of the Higgs boson to massive bottom quarks at order α_s^3* , *JHEP* **03** (2025) 163, [2411.07493].
- [15] A. B. Goncharov, *Multiple polylogarithms, cyclotomy and modular complexes*, *Math. Res. Lett.* **5** (1998) 497–516, [1105.2076].
- [16] T. Liu and A. Penin, *High-Energy Limit of Mass-Suppressed Amplitudes in Gauge Theories*, *JHEP* **11** (2018) 158, [1809.04950].
- [17] T. Liu, S. Modi and A. A. Penin, *Higgs boson production and quark scattering amplitudes at high energy through the next-to-next-to-leading power in quark mass*, *JHEP* **02** (2022) 170, [2111.01820].

- [18] K. G. Chetyrkin and M. Steinhauser, *Complete QCD corrections of order $O(\alpha_s^3)$ to the hadronic Higgs decay*, *Phys. Lett. B* **408** (1997) 320–324, [[hep-ph/9706462](#)].
- [19] S. A. Larin, T. van Ritbergen and J. A. M. Vermaseren, *The Large top quark mass expansion for Higgs boson decays into bottom quarks and into gluons*, *Phys. Lett. B* **362** (1995) 134–140, [[hep-ph/9506465](#)].
- [20] K. G. Chetyrkin, J. H. Kuhn and M. Steinhauser, *RunDec: A Mathematica package for running and decoupling of the strong coupling and quark masses*, *Comput. Phys. Commun.* **133** (2000) 43–65, [[hep-ph/0004189](#)].
- [21] F. Herren and M. Steinhauser, *Version 3 of RunDec and CRunDec*, *Comput. Phys. Commun.* **224** (2018) 333–345, [[1703.03751](#)].
- [22] C. Anastasiou, C. Duhr, F. Dulat, F. Herzog and B. Mistlberger, *Higgs Boson Gluon-Fusion Production in QCD at Three Loops*, *Phys. Rev. Lett.* **114** (2015) 212001, [[1503.06056](#)].